

Criticality and the fractal structure of $-5/3$ turbulent cascades

Juan Luis Cabrera,^{1,2,3,*} Esther D. Gutiérrez,^{4,2,3} and Miguel Rodríguez Márquez^{5,3}

¹*Departamento de Física Aplicada, ETSI Aeronáutica y del Espacio,
Universidad Politécnica de Madrid,
Pza. Cardenal Cisneros 3, 28040, Madrid, Spain*

²*Laboratorio de Dinámica Estocástica, Centro de Física,
Instituto Venezolano de Investigaciones Científicas, Caracas 1020-A, Venezuela*

³*Deeptikus Ltd., 10A Tasman Ave.,
Mount Albert, Auckland 1025, New Zealand*

⁴*Facultad de Ciencias Naturales y Matemáticas,
Escuela Superior Politécnica del Litoral,
Km 30.5 Vía Perimetral, Guayaquil, Ecuador*

⁵*Departamento de Ciencias Naturales y Exactas,
Corporación Universidad de la Costa,
Calle 58 No. 55-66, Barranquilla, Colombia*

(Dated: March 17, 2021)

Abstract

Here we show a procedure to generate an analytical structure producing a cascade that scales as the energy spectrum in isotropic homogeneous turbulence. We obtain a function that unveils a non-self-similar fractal at the origin of the cascade. It reveals that the backbone underlying $-5/3$ cascades is formed by deterministic nested polynomials with parameters tuned in a Hopf bifurcation critical point. The cascade scaling is exactly obtainable (not by numerical simulations) from deterministic low dimensional nonlinear dynamics. Consequently, it should not be exclusive for fluids but also present in other complex phenomena. The scaling is obtainable both in deterministic and stochastic situations.

Keywords: Cascade, criticality, fractals, nonlinear, stochastic, turbulence, maps, complex.

* julusca@gmail.com

I. INTRODUCTION

Low dimensional dynamical systems have played a central role in our understanding of the transition to turbulence in hydrodynamical systems [1, 2] and provided a background to study turbulence [3–5]. As L.P. Kadanoff once pointed out, the use of a simple system in hydrodynamics is similar to its use in critical phenomena in condensed matter physics, where it allows to understand complicated phase transitions because it shows qualitatively similar changes [2]. The analysis of the simple system allows the extraction of universal features that are also found in the more complex problem. A remarkable example of such an approach has been using the logistic equation [6], to explain the period doubling route to turbulence [2, 7, 8]. Unfortunately, in spite of that insight and many others, turbulence still remains an open problem.

In this paper we are concerned with the energy cascade observed in fully developed turbulence and characterized by a $-5/3$ power law spectrum. Inspired by the idea of a cascade advanced previously by Richardson [9], and based on a clever analysis, the scaling law was obtained by Kolmogorov [10], Onsager [11] and others [12–14]. Nevertheless, a detailed description of the underlying process that governs the flow of energy, through the different scales involved in a turbulent cascade, has yet to be found. We analyze a particular low dimensional system and obtain an analytical structure that describes a branching process yielding the $-5/3$ power law. This outcome is the result of an exact calculation, not using a numerical simulation.

II. THE DRM

We study a well known low dimensional dynamics that - as is the case of the logistic equation - is originated in population biology [15]. Let's consider an stochastic version of the delayed regulation model (DRM), given by the map on the unit interval, $x \in [0, 1]$,

$$x_{g+1} = r_g x_g (1 - x_{g-1}), \quad (1)$$

where $g = 1, \dots, +\infty$, is an iteration index we will call generation, $r_g = a\eta_g + b$, with η_g some random perturbation indexed by g ; a , the intensity and b a bias parameter. For simplicity sake we assume the simplest case with η_g uniformly distributed on $[0, 1]$, so that $r_g \in [b, a+b]$. For the case of zero delay and zero noise, the map (1) is the deterministic logistic map. Eq.

(1) is one of the simplest dynamical systems containing nonlinearities, time delayed feedback and parametric random perturbations. The deterministic counterpart of Eq. (1) has been widely studied [16–18] and its non-deterministic version has been used to analyze stochastic extinction [19–21], autonomous stochastic resonance [22] and noise-induced localization [23]. Eq. (1) shows sustained on-off intermittency caused by destabilization of the origin and by destabilization of the fixed point $1 - 1/\langle r_g \rangle$, where the intermittent temporal series contains bursts involving stochastic limit cycle oscillations. The DRM undergoes a Hopf bifurcation at $r_H = 2$ [18, 20, 21].

III. LINEALIZATION OF THE DRM

In the following, we will utilize noise to help with the calculations. It will allow us to obtain simple expressions which in turn will lead us to the main results. Later, such results will be analyzed with and without noise. The first step consist in the linearization of Eq. (1), which is rewritten as,

$$x_{g+1} = r_g F(x_g, y_g) \quad (2)$$

$$y_{g+1} = G(x_g, y_g), \quad (3)$$

with $F(x, y) \equiv x(1 - y)$ and $G(x, y) \equiv x$. F and G can be expanded around the fixed point $P \equiv (\alpha, \alpha)$, with $\alpha \equiv 1 - \frac{1}{\langle r_g \rangle} \equiv 1 - \frac{1}{\beta}$, to obtain,

$$F(x, y) = F(\alpha, \alpha) + (x - \alpha) \frac{\partial F}{\partial x} \Big|_P + (y - \alpha) \frac{\partial F}{\partial y} \Big|_P + O(x^2, y^2) \quad (4)$$

$$G(x, y) = G(\alpha, \alpha) + (x - \alpha) \frac{\partial G}{\partial x} \Big|_P + (y - \alpha) \frac{\partial G}{\partial y} \Big|_P + O(x^2, y^2), \quad (5)$$

i.e.,

$$F(x, y) = \alpha^2 + (1 - \alpha)x - \alpha y \quad (6)$$

$$G(x, y) = x. \quad (7)$$

Close to the fixed point P , Eq. (1) can be approximated by its linear part:

$$x_{g+1} = r_g \left(\alpha^2 + \frac{x_g}{\beta} - \alpha y_g \right) \quad (8)$$

$$y_{g+1} = x_g \quad (9)$$

And it is better to rewrite it as,

$$\begin{pmatrix} x \\ y \end{pmatrix}_{g+1} = \begin{pmatrix} r_g/\beta & -\alpha r_g \\ 1 & 0 \end{pmatrix} \begin{pmatrix} x \\ y \end{pmatrix}_g + \begin{pmatrix} \alpha^2 r_g \\ 0 \end{pmatrix}. \quad (10)$$

So we can define the evolution matrix:

$$\mathbf{A}_g \equiv \begin{pmatrix} r_g/\beta & -\alpha r_g \\ 1 & 0 \end{pmatrix}, \quad (11)$$

and the bias vector:

$$\vec{B}_g \equiv \begin{pmatrix} \alpha^2 r_g \\ 0 \end{pmatrix}. \quad (12)$$

Then, Eq. (10) can be compacted as,

$$\vec{X}_{g+1} = \mathbf{A}_g \vec{X}_g + \vec{B}_g. \quad (13)$$

IV. EXPANDING \vec{X}_g

It is useful to express \vec{X}_g in terms of the initial state \vec{X}_0 . So, let's note that \vec{X}_{g+1} can be patiently expanded as follows,

$$\begin{aligned} \vec{X}_{g+1} &= \mathbf{A}_g \vec{X}_g + \vec{B}_g \\ &= \mathbf{A}_g (\mathbf{A}_{g-1} \vec{X}_{g-1} + \vec{B}_{g-1}) + \vec{B}_g \\ &= \mathbf{A}_g (\mathbf{A}_{g-1} (\mathbf{A}_{g-2} \vec{X}_{g-2} + \vec{B}_{g-2}) + \vec{B}_{g-1}) + \vec{B}_g \\ &\quad \vdots \\ &= \mathbf{A}_g \mathbf{A}_{g-1} \mathbf{A}_{g-2} \mathbf{A}_{g-3} \dots \mathbf{A}_1 \mathbf{A}_0 \vec{X}_0 \\ &\quad + \mathbf{A}_g \mathbf{A}_{g-1} \mathbf{A}_{g-2} \mathbf{A}_{g-3} \dots \mathbf{A}_1 \vec{B}_0 \\ &\quad \vdots \\ &\quad + \mathbf{A}_g \mathbf{A}_{g-1} \mathbf{A}_{g-2} \vec{B}_{g-3} \\ &\quad + \mathbf{A}_g \mathbf{A}_{g-1} \vec{B}_{g-2} \\ &\quad + \mathbf{A}_g \vec{B}_{g-1} \\ &\quad + \vec{B}_g \end{aligned} \quad (14)$$

So, \vec{X}_{g+1} can be written as,

$$\begin{aligned}
\vec{X}_{g+1} &= \prod_{j=0}^g \mathbf{A}_{\mathbf{g}-j} \vec{X}_0 \\
&+ \prod_{j=0}^{g-1} \mathbf{A}_{\mathbf{g}-j} \vec{B}_0 \\
&+ \prod_{j=0}^{g-2} \mathbf{A}_{\mathbf{g}-j} \vec{B}_1 \\
&+ \prod_{j=0}^{g-3} \mathbf{A}_{\mathbf{g}-j} \vec{B}_2 \\
&\vdots \\
&+ \prod_{j=0}^{g-(g-2+1)=1} \mathbf{A}_{\mathbf{g}-j} \vec{B}_{g-2} \\
&+ \prod_{j=0}^{g-(g-1+1)=0} \mathbf{A}_{\mathbf{g}-j} \vec{B}_{g-1} \\
&+ \vec{B}_g \\
&= \prod_{j=0}^g \mathbf{A}_{\mathbf{g}-j} \vec{X}_0 \\
&+ \sum_{i=1}^{g+1} \prod_{j=0}^{g-i} \mathbf{A}_{\mathbf{g}-j} \vec{B}_{i-1}.
\end{aligned} \tag{15}$$

Where we are using the definition,

$$\prod_{j=0}^{g-i} \mathbf{A}_{\mathbf{g}-j} \equiv 1 \text{ if } i = g + 1. \tag{16}$$

Now, changing variables, $g \longrightarrow g' - 1$, we obtain,

$$\vec{X}_g = \prod_{j=0}^{g-1} \mathbf{A}_{\mathbf{g}-j-1} \vec{X}_0 + \sum_{i=1}^g \prod_{j=0}^{g-i-1} \mathbf{A}_{\mathbf{g}-j-1} \vec{B}_{i-1}, \tag{17}$$

where we have omitted the prime and used,

$$\prod_{j=0}^{g-i-1} \mathbf{A}_{\mathbf{g}-j-1} \equiv 1 \text{ if } i = g. \tag{18}$$

Thus, we can define,

$$\mathbf{P}_i \equiv \prod_{j=0}^{g-i-1} \mathbf{A}_{\mathbf{g}-j-1} \quad \text{if } i \neq g, \tag{19}$$

$$\mathbf{P}_i \equiv \mathbf{1} \quad \text{if } i = g,$$

$$\mathbf{P}_g \equiv \prod_{j=0}^{g-1} \mathbf{A}_j, \tag{20}$$

to write \vec{X}_g in a compact form,

$$\vec{X}_g = \mathbf{P}_g \vec{X}_0 + \sum_{i=1}^g \mathbf{P}_i \vec{B}_{f(i)}, \quad (21)$$

with $f(i) \equiv i - 1$.

V. SIMPLIFYING $\vec{X}_g = \mathbf{P}_g \vec{X}_0 + \sum_{i=1}^g \mathbf{P}_i \vec{B}_{f(i)}$

For convenience, the following calculations are carried out on the complex plane. Here we want to simplify the expression (21) as much as possible. So, let be \vec{Y}_g a state at generation g , obtained with a realization $r'_g \neq r_g$. Calculating the dot product of \vec{X}_g and \vec{Y}_g gives,

$$\vec{X}_g \cdot \vec{Y}_g = \mathbf{P}_g \vec{X}_0 \cdot \vec{Y}_g + \sum_{i=1}^g \mathbf{P}_i \vec{B}_{f(i)} \cdot \vec{Y}_g. \quad (22)$$

The scalar quantity, $\eta_g \equiv \vec{X}_g \cdot \vec{Y}_g$, is the value for the projection of \vec{X}_g onto \vec{Y}_g . It is a random variable evaluated at generation g , that takes values on the interval $[0, 1]$. Also, let's note that applying the operator \mathbf{P}_g on the initial condition \vec{X}_0 , produces a new state at generation g , say $\vec{\mu}_g$. Thus, the dot product between $\mathbf{P}_g \vec{X}_0 = \vec{\mu}_g$ and \vec{Y}_g yields also a scalar random variable at generation g , say $0 \leq \psi_g \leq 1$, i.e.,

$$\mathbf{P}_g \vec{X}_0 \cdot \vec{Y}_g = \vec{\mu}_g \cdot \vec{Y}_g \equiv \psi_g \quad (23)$$

With these considerations in mind we can rewrite Eq. (22) as,

$$\begin{aligned} \eta_g &= \psi_g + \sum_{i=1}^g \mathbf{P}_i \vec{B}_{f(i)} \cdot \vec{Y}_g \\ &= \psi_g \left(1 + \psi_g^{-1} \sum_{i=1}^g \mathbf{P}_i \vec{B}_{f(i)} \cdot \vec{Y}_g \right). \end{aligned} \quad (24)$$

After rearranging terms, it results in,

$$\psi_g \left(\frac{\eta_g}{\psi_g} - 1 \right) = \sum_{i=1}^g \mathbf{P}_i \vec{B}_{f(i)} \cdot \vec{Y}_g \quad (25)$$

or

$$\left(\frac{\eta_g}{\psi_g} - 1 \right) \vec{\mu}_g \cdot \vec{Y}_g = \sum_{i=1}^g \mathbf{P}_i \vec{B}_{f(i)} \cdot \vec{Y}_g, \quad (26)$$

where we have used Eq. (23). This expression is the same as,

$$\left\{ \left(\frac{\eta_g}{\psi_g} - 1 \right) \vec{\mu}_g - \sum_{i=1}^g \mathbf{P}_i \vec{B}_{f(i)} \right\} \cdot \vec{Y}_g = 0. \quad (27)$$

Now, at a given step g , this equation has two possible consequences: i) either the vectors, $\left(\left(\frac{\eta_g}{\psi_g} - 1\right) \vec{\mu}_g - \sum_{i=1}^g \mathbf{P}_i \vec{B}_{f(i)}\right)$ and \vec{Y}_g , are orthogonal vectors, in which case its dot product would equal zero, or ii) the following equality is satisfied,

$$\left(\frac{\eta_g}{\psi_g} - 1\right) \vec{\mu}_g = \sum_{i=1}^g \mathbf{P}_i \vec{B}_{f(i)}, \quad (28)$$

In what follows, we assume that condition ii) predominates, i.e., that the involved random dynamics reduces the probability of i) to a minimum, such that most of the evolution of the system can be better characterized by condition ii) at least in $O(\{(\frac{\eta_g}{\psi_g} - 1) \vec{\mu}_g - \sum_{i=1}^g \mathbf{P}_i \vec{B}_{f(i)}\} \cdot \vec{Y}_g)$. That being said, we must also impose $b > 1$, to avoid the case $r_g < 1$ if $\eta_g = 0$, which would take the system state to the zero fixed point, a situation where we can't rule out $\vec{Y}_g = 0$, at least momentarily. With these thoughts in mind, and using the definition of $\vec{\mu}_g$, condition ii) turns out as,

$$\left(\frac{\eta_g}{\psi_g} - 1\right) \mathbf{P}_g \vec{X}_0 = \sum_{i=1}^g \mathbf{P}_i \vec{B}_{f(i)}, \quad (29)$$

a relation that we can introduce into Eq. (21), to obtain a shorter expression for the time evolution of the system in terms of the product \mathbf{P}_g ,

$$\begin{aligned} \vec{X}_g &= \mathbf{P}_g \vec{X}_0 + \left(\frac{\eta_g}{\psi_g} - 1\right) \mathbf{P}_g \vec{X}_0, \\ &= \frac{\eta_g}{\psi_g} \mathbf{P}_g \vec{X}_0 \\ &= \gamma_g \mathbf{P}_g \vec{X}_0 \\ &= \mathbf{P}'_g \vec{X}_0. \end{aligned} \quad (30)$$

Here, $\gamma_g \equiv \frac{\eta_g}{\psi_g}$, is a new random number and $\mathbf{P}'_g \equiv \gamma_g \mathbf{P}_g$ is the original product modulated by γ_g . To know the range of values that γ_g takes on, let's consider the inequality:

$$0 \leq \mathbf{P}_g \vec{X}_0 \cdot \vec{Y}_g < \mathbf{P}_g \vec{X}_0 \cdot \vec{Y}_g + \sum_{i=1}^g \mathbf{P}_i \vec{B}_{f(i)} \cdot \vec{Y}_g = \vec{X}_g \cdot \vec{Y}_g \leq 1 \quad (31)$$

or

$$0 \leq \mathbf{P}_g \vec{X}_0 \cdot \vec{Y}_g < \vec{X}_g \cdot \vec{Y}_g \leq 1, \quad (32)$$

i.e.,

$$0 \leq \psi_g < \eta_g \leq 1. \quad (33)$$

Then,

$$1 < \gamma_g < \infty. \quad (34)$$

Consequently, γ_g is an unbounded random variable larger than 1, i.e., applying γ_g on \mathbf{P}_g has an amplifying effect.

VI. CALCULATING THE NORM OF \vec{X}_g

At this point, we would like to know about the behavior of the norm of \vec{X}_g . Such a quantity can be determined calculating the following inner product,

$$\|\vec{X}_g\| = [\vec{X}_g^* \vec{X}_g]^{1/2} = [\vec{X}_0 \mathbf{P}'_g \mathbf{P}_g \vec{X}_0]^{1/2}, \quad (35)$$

given that \mathbf{P}'_g is not a self-adjoint operator. Here \mathbf{P}'_g is the Hermitian conjugate of the operator \mathbf{P}_g , i.e., the adjoint matrix in our case. Then, the problem of calculating the norm translates to the calculation of $\mathbf{P}'_g \mathbf{P}_g$. To evaluate such a product we must write it in terms of the time dependent random matrix \mathbf{A}_g ,

$$\mathbf{P}'_g \mathbf{P}_g = \gamma_g^* \mathbf{P}_g^\dagger \gamma_g \mathbf{P}_g = \gamma_g^* \gamma_g \mathbf{P}_g^\dagger \mathbf{P}_g, \quad (36)$$

where

$$\begin{aligned} \mathbf{M}_g \equiv \mathbf{P}_g^\dagger \mathbf{P}_g &= [\mathbf{A}_{g-1} \mathbf{A}_{g-2} \dots \mathbf{A}_1 \mathbf{A}_0]^\dagger \mathbf{A}_{g-1} \mathbf{A}_{g-2} \dots \mathbf{A}_1 \mathbf{A}_0 = \\ &= \mathbf{A}_0^\dagger \mathbf{A}_1^\dagger \dots \mathbf{A}_{g-2}^\dagger \mathbf{A}_{g-1}^\dagger \mathbf{A}_{g-1} \mathbf{A}_{g-2} \dots \mathbf{A}_1 \mathbf{A}_0 = \\ &= \mathbf{A}_0^\dagger [\mathbf{A}_1^\dagger \dots [\mathbf{A}_{g-2}^\dagger [\mathbf{A}_{g-1}^\dagger \mathbf{A}_{g-1}] \mathbf{A}_{g-2}] \dots \mathbf{A}_1] \mathbf{A}_0, \end{aligned} \quad (37)$$

and

$$\mathbf{A}_g^\dagger = \begin{pmatrix} r_g/\beta & 1 \\ -r_g\alpha & 0 \end{pmatrix} \quad (38)$$

VII. EIGENVALUES OF p_1

A straightforward evaluation of \mathbf{M}_g doesn't seem plausible. However, we can address our attention on its step by step evolution. In particular, in the equation for \mathbf{M}_g , the core or first product is given by:

$$p_1 \equiv \mathbf{A}_{g-1}^\dagger \mathbf{A}_{g-1} = \begin{pmatrix} \frac{r_1^2 + \beta^2}{\beta^2} & -\frac{r_1^2}{\beta} \alpha \\ -\frac{r_1^2}{\beta} \alpha & \alpha^2 r_1^2 \end{pmatrix}, \quad (39)$$

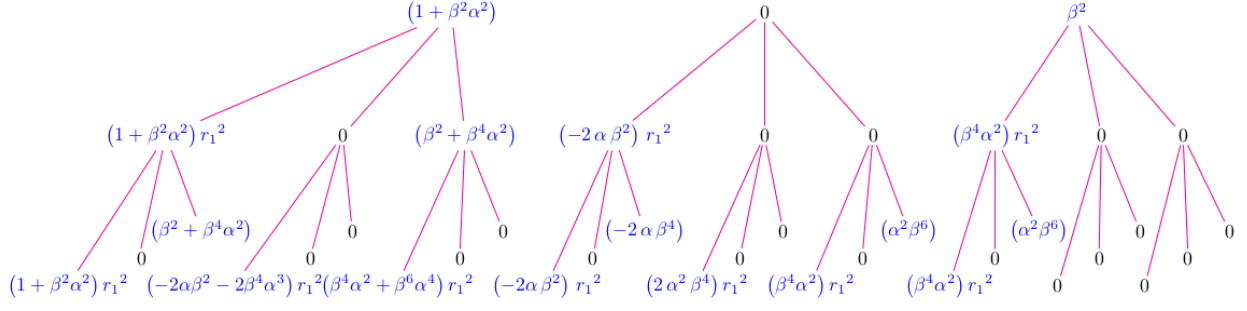


FIG. 1. Tree representation for the generation of the polynomial coefficients after two iterations of rule (49, 50), starting from Λ_1 . Bottom coefficients are those forming Λ_3 given by Eq. (B3).

where we are using the notation $r_i \equiv r_{g-i}$. It should be noted that this matrix has eigenvalues,

$$\lambda_{\pm}^{p_1} = \frac{1}{2\beta^2} \left((1 + \alpha^2 r_1^2) \beta^2 + r_1^2 \pm \sqrt{((1 + \alpha^2 r_1^2) \beta^2 + r_1^2)^2 - (2\alpha\beta^2 r_1)^2} \right). \quad (40)$$

So, the eigenvalues of the product p_1 can be expressed as,

$$\lambda_{\pm}^{p_1} = \frac{1}{2\beta^2} \left(\Lambda_1 \pm \sqrt{\Lambda_1^2 - \Upsilon_1^2} \right). \quad (41)$$

where, $\Lambda_1 \equiv (1 + \beta^2 \alpha^2) r_1^2 + \beta^2$, and $\Upsilon_1 \equiv 2\beta^2 \alpha r_1$. This process is repeated to calculate the next product, $p_2 \equiv \mathbf{A}_{g-2}^\dagger p_1 \mathbf{A}_{g-2}$, and similarly, p_3 , and so on. A detailed account of these calculations is provided in the appendixes A-D. From there, it is clear that the eigenvalues for the first five products can be expressed as:

$$\lambda_{\pm}^{p_2} = \frac{1}{2\beta^4} \left(\Lambda_2 \pm \sqrt{\Lambda_2^2 - \Upsilon_2^2} \right) \quad (42)$$

$$\lambda_{\pm}^{p_3} = \frac{1}{2\beta^6} \left(\Lambda_3 \pm \sqrt{\Lambda_3^2 - \Upsilon_3^2} \right) \quad (43)$$

$$\lambda_{\pm}^{p_4} = \frac{1}{2\beta^8} \left(\Lambda_4 \pm \sqrt{\Lambda_4^2 - \Upsilon_4^2} \right) \quad (44)$$

$$\lambda_{\pm}^{p_5} = \frac{1}{2\beta^{10}} \left(\Lambda_5 \pm \sqrt{\Lambda_5^2 - \Upsilon_5^2} \right) \quad (45)$$

where the definitions for Λ_i and Υ_i are given in the appendixes.

VIII. NESTED STRUCTURES

The previous section allows us to infer how the eigenvalues evolve with each generation g . In particular, the eigenvalues for the products, p_1, p_2, \dots, p_N , can be written as,

$$\lambda_{\pm}^{p_g} = \frac{1}{2\beta^{2g}} \left(\Lambda_g \pm \sqrt{\Lambda_g^2 - \Upsilon_g^2} \right), \quad (46)$$

where terms Λ_g and Υ_g are polynomials in the noise terms, i.e., random polynomials. In particular, Υ_g , can be easily written in compact form as,

$$\Upsilon_g = 2\beta^{2g}\alpha^g \prod_{i=1}^g r_i. \quad (47)$$

However, a closed form for Λ_g can not be obtained so easily. It is so because Λ_g follows a complex nested structure as is illustrated in the appendixes. One must note that Λ_g is a polynomial in r_g of order two, which coefficients are polynomials of order two in r_{g-1} , which coefficients are polynomials of order two in r_{g-2} , and so on. So, let's say that $C(r_{g-1}, \dots, r_1)$ is a function that depends on the noise terms r_{g-1}, \dots, r_1 , and that such a function is a coefficient of a noise term of order i , i.e., that given a second order polynomial describing Λ_g it has terms $C_i(r_{g-1}, \dots, r_1)r^i$. Now, depending on what Λ_g are we dealing with, we shall distinguish each of these functional coefficients. Consequently, it is convenient indexing also the C 's to make such a distinction, so writing these terms as $C_{g,i}(r_{g-1}, \dots, r_1)r_g^i$. Here, we have also indexed r_g , because that noise's value is exactly the one at step g . Accordingly, Λ_g can be conveyed to,

$$\Lambda_g = \sum_{i=0}^2 C_{g,i}(r_{g-1}, \dots, r_1)r_g^i \quad (48)$$

with $C_{1,i} \equiv C_{g,i}(r_{g-1}, \dots, r_1)|_{g=1}$, constant. Note that we have not indexed the coefficients of the nested levels because there is no need for that, we try to keep the notation simple, as far as possible. Now, let's reproduce the full structure as follows. In general, if we know Λ_1 and Λ_2 , we can obtain Λ_g given that, in the generation $g - 1$, a given term,

$$\left\{ C_2 r_i^2 + C_1 r_i + C_0 \right\} r_{i+1}^k \quad \text{with } k = 0, 1, 2, \quad (49)$$

generates the polynomial,

$$\left\{ \begin{array}{l} [C_2 r_i^2 + C_1 \chi_1 r_i + \beta^2 C_2] r_{i+1}^2 \\ + [-k\alpha\beta^2 C_2 r_i^2 + C_1 \chi_2 r_i + C_1 \chi_3] r_{i+1} \\ + [\beta^2 \alpha^2 C_0 r_i^2 + C_1 \chi_4 r_i + C_1 \chi_5] \end{array} \right\} r_{i+2}^k, \quad (50)$$

in the next generation, g . $\chi_1, \chi_2, \dots, \chi_5$ are unknowns, here included to stress the polynomial nested structure, but multiplied by C_1 , that in the present situation vanishes.

IX. GENERATING NESTED ESTRUCTURES: AN EXAMPLE

The preceding procedure is better illustrated with an example: finding Λ_3 from Λ_2 , which is given by Eq. (A3). The coefficient for the quadratic term is, $[(1 + \alpha^2\beta^2)r_1^2 + \beta^2(1 + \alpha^2\beta^2)]$, therefore, $C_2 = 1 + \alpha^2\beta^2$, $C_1 = 0$ and $C_0 = \beta^2(1 + \alpha^2\beta^2)$; and the quadratic term in r_3 is generated as,

$$\left\{ \begin{array}{l} [(1 + \alpha^2\beta^2)r_1^2 + \beta^2(1 + \alpha^2\beta^2)] r_2^2 \\ + [-2\alpha\beta^2(1 + \alpha^2\beta^2)r_1^2] r_2 \\ + [\beta^4\alpha^2(1 + \alpha^2\beta^2)r_1^2] \end{array} \right\} r_3^2. \quad (51)$$

Now, the lineal term in Λ_2 is $-2\alpha\beta^2r_1^2$, therefore in this case, $C_2 = -2\alpha\beta^2$ and $C_1 = C_0 = 0$.

Then the linear term in r_3 is,

$$\left\{ \begin{array}{l} [(-2\alpha\beta^2)r_1^2 + (-2\alpha\beta^4)] r_2^2 \\ + [2\alpha^2\beta^4r_1^2] r_2 \end{array} \right\} r_3. \quad (52)$$

Finally, the coefficient of the independent term in Λ_2 is $(\alpha^2\beta^4)r_1^2$. Then $C_2 = \alpha^2\beta^4$ and $C_1 = C_0 = 0$, so we obtain,

$$\left\{ [(\alpha^2\beta^4)r_1^2 + \alpha^2\beta^6] r_2^2 \right\} r_3^0. \quad (53)$$

Adding Eq. (51), (52) and (53) results in Λ_3 .

X. DETERMINING THE LEADING TERM IN λ

The eigenvalues of \mathbf{M}_g are given by Eq. (46) with the term Υ_g growing as a power of the noise term, i.e., $\Upsilon_g \sim r^g$. Meanwhile, the equations (VII), (A3), (B3), (C3) and (D3) indicate that the Λ_g 's grow as a sum of powers in the noise, i.e.,

$$\begin{aligned} \Lambda_1 &\sim r^2 \\ \Lambda_2 &\sim r^4 + r^3 + r^2 \\ \Lambda_3 &\sim r^6 + r^5 + r^4 + r^3 + r^2 \\ \Lambda_4 &\sim r^8 + r^7 + r^6 + r^5 + r^4 \\ \Lambda_5 &\sim r^{10} + \dots + r^4. \end{aligned} \quad (54)$$

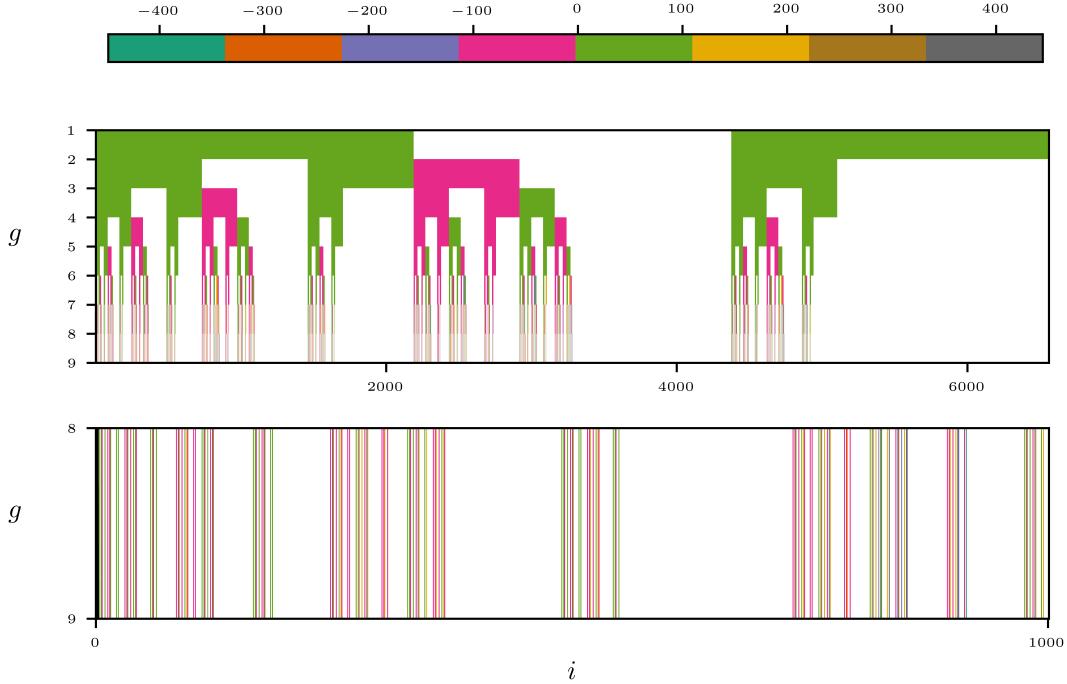


FIG. 2. (Top) Analytical deterministic cascade describing the evolution of the nested polynomial coefficients C_2 , C_1 and C_0 (from left to right) after $n = 8$ iterations. Colors represent the coefficient's intensities a_i . The iteration process starts with the Λ_1 coefficients, each one laying on $\frac{1}{3}$ segments on the x -axis which hosts 3^8 subdivisions. (Bottom) Zoom in the interval $[0, 1000]$ showing fine structure. Parameter values are $r = 1$, $a = 0.085$ and $b = 1.9375$.

So, $\Lambda_g > \Upsilon_g$ and Λ_g will predominate for g sufficiently large, i.e., $\frac{\Upsilon_g}{\Lambda_g} \rightarrow 0$, thus Eq. (46) yields,

$$\begin{aligned} \lambda_+^{p_g} &\sim \Lambda_g + O\left(\frac{\Upsilon_g}{\Lambda_g}\right) \\ \lambda_-^{p_g} &\sim 0 + O\left(\frac{\Upsilon_g}{\Lambda_g}\right) \end{aligned} \quad (55)$$

Let's unpack Eq. (35) to determine the implications of this approximation on the norm $\|\vec{X}_g\|$,

$$\begin{aligned} \|\vec{X}_g\| &= (\gamma_g^* \gamma_g \vec{X}_0^* \mathbf{M}_g \vec{X}_0)^{1/2} \\ &= \gamma_g \left[(x_0 y_0) \begin{pmatrix} \lambda_+ & 0 \\ 0 & \lambda_- \end{pmatrix} \begin{pmatrix} x_0 \\ y_0 \end{pmatrix} \right]^{\frac{1}{2}}. \end{aligned} \quad (56)$$

Combining this equation with the Eqs. (55) we find that Λ_g leads the behavior of the norm,

$$\|\vec{X}_g\| \sim \frac{\gamma_g}{\beta^g} \sqrt{\Lambda_g} x_0. \quad (57)$$

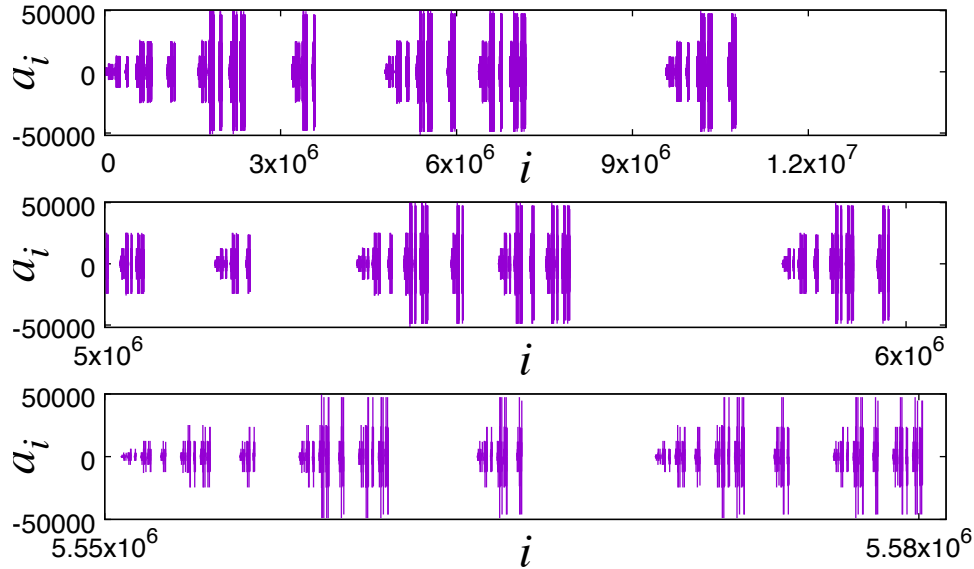


FIG. 3. Non-self-similar structure of the analytical deterministic cascade revealed after successive enlargements. Image obtained with $g = 15$ generations and parameter values as in figure 2. The number of coefficients calculated is $3^{15} = 14348907$. Points are represented by impulses and zero ones have been extracted.

XI. A HIDDEN FRACTAL STRUCTURE

The hidden structure of the Λ_g 's is better understood using a graphical representation. Figure 1 shows the branching process obtained after three iterations of the rule (49, 50). The terms displayed at the bottom are the coefficients of Λ_3 (see Appendix B). This representation reveals a cascading process at the backbone of the eigenvalues time evolution. To get a deeper insight into such a structure we will focus exclusively on the evolution of the coefficients described in figure 1, turning off any random modulation. It is achieved, arbitrarily considering $r_g = r$, a constant, conveniently established as $r = 1, \forall g$. Therefore, now the magnitude of the coefficients depends only on the values of a and b which will be chosen such that $(a + b)$ is close to the Hopf bifurcation parameter value $r_H = 2$. This procedure allows us to separate the contribution of the coefficients exclusively as in figure

1. Under these conditions the cascade obtained is depicted in figure 2. The method used to obtain this figure is as follows: the coefficient values in the initial polynomial Λ_1 , i.e., C_2 , C_1 and C_0 , define branch intensities, a_i , $i = 1, 2, 3$, on the $N_1 = 3^1$ subintervals of the unit interval: $I_2 \equiv [0, \frac{1}{3})$, $I_1 \equiv [\frac{1}{3}, \frac{2}{3})$ and $I_0 \equiv [\frac{2}{3}, 1]$, respectively. After one iteration, each subset is divided by a factor of 3, and the newly generated coefficients - obtained using rule (49, 50) - shall update the a_i 's on the new $N_2 = 3^2$ subintervals. After each new generation, the unit interval is divided by a factor of 3 such that, after g iterations, the value of the coefficients can be represented as intensities on $N_g = 3^g$ subintervals, given by rule (49, 50). Figure 2 shows how fast the cascade grows: after $g = 8$ generations, the unit interval harbours $N_8 \sim 3^8 = 6561$ coefficients on the same number of subintervals. Because $r_g = 1$, $\forall g$, this fractal cascade is the support for random perturbations to shape the norm of \vec{X}_g or other dynamical quantities grounded on it. The bottom part of figure 2 shows a detail of the fine structure of that object. I_2 is the only segment that obeys a self-similar rule, given by $X_{g+1} = \frac{X_g}{3}$; $X \in I = [0, 1]$. Subintervals I_1 and I_0 don't seem to follow a self-similar rule. The mapping process shows an independent progression for each of the initial I_i intervals, yielding a non-self-similar structure with multifractal characteristics whose full characterization will be carried out elsewhere. Branch intensities a_i , $i = 1 \dots 3^g$, display a nontrivial behaviour as seen in figure 3. We plotted a_i for each branch on the limit set after $g = 15$ iterations. The horizontal axis contains $N_{15} = 3^{15} = 14348907$ points. Successive enlargements of the initial interval show statistically equivalent objects as expected for a fractal. The figure also shows that the lack of self-similarity extends to both, the branch positions and their intensities. The behavior of the distribution of intensities (figure 4) is comparable with Thomae's self-similar function as has been reported also for high-throughput biological and clinical data [24].

XII. CASCADING SCALING BEHAVIOUR

So far, except for using the term cascade to describe successive iterations of rule (49, 50), we haven't shown any link with cascades in turbulence phenomena. To establish such a bridge, we must conjecture some sort of parallel between the intensities a_i and the energy by wave number. The idea behind this is that, if a_i is a main changing quantity from the cascading rule (49, 50), it could be related with a main changing quantity in turbulent

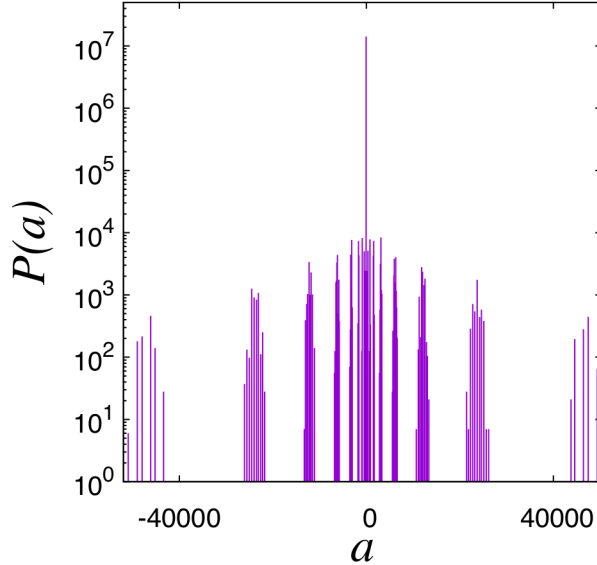


FIG. 4. Semi-log plot of the intensity distribution from the deterministic cascade obtained after 15 generations. Same parameter values as in figure 2.

cascades: the energy, i.e.,

$$E(k) \sim E(a_i(g)). \quad (58)$$

Thus, we advance the following definition: if there are l_g non-zero intensities at a scale g , we define an energy measure at generation step g by the relation:

$$E(a_i(l_g)) \equiv \left(\sum_{\forall a_i \neq 0} |a_i(l_g)| \right)^{-1}, \quad (59)$$

i.e., the inverse value of the summation of the magnitude for all intensities at scale g . Circles shown in figure 5(left) describe the behavior of this quantity as a function of the scale, for a deterministic cascade as the one illustrated in figure 2, and obtained with r close to the Hopf bifurcation point. It can be seen that $E(a_i(l_g))$ obey a $-5/3$ power law over six orders of magnitude. This is the same power law found for the energy spectrum in fully developed isotropic homogeneous turbulence [25]. Therefore, $E(l_g)$ scales following the expected law for turbulent cascades,

$$E(l_g) \sim l_g^{-\frac{5}{3}}. \quad (60)$$

From this relation, it is straightforward to identify l_g with the wave number k at a given scale, i.e., $l_g \sim k$. Thus, assumption (58) can be explicitly written as,

$$E(k) \sim E(l_g) \sim l_g^{-\frac{5}{3}}. \quad (61)$$

When the parameter values are distant from the bifurcation critical point, the calculated $E(l_g)$ deviates from the $-5/3$ power law, as is shown in figure 5(left). The cascading rule (49, 50) resembles a turbulent cascade exclusively when the parameter r is almost tuned on the Hopf bifurcation critical point and such resemblance disappears when the parameter is moved away from it. This result emphasizes a critical and deterministic origin of the cascade's $-5/3$ power law. Our results suggest that in this deterministic situation, the cascade would continue without end, meaning that increasing g to a much larger value shall still produce the $-5/3$ law, in which case one could assume that the inertial range extends to infinity. Such an assumption is in line with Onsager's conjecture that dissipation energy might exist even in the limit of vanishing viscosity [11, 26]. Additionally, an interesting characteristic of the cascade reported here is that it is rooted in an apparently multifractal structure.

Next, we consider the situation when a uniform noise is turned on. Results for this case are shown in the figure 5(right). We found that, after averaging over realizations, $E(a_i(l_g))$ also follows a $-5/3$ power law, i.e., the analytical cascade behaves on the average as a turbulent system. Nevertheless, some comments are in order: circle points were calculated for 100 noise realizations. For large generations (larger l_g) the calculated values for $E(a_i(l_g))$ depart from the power law. In spite in this region most of the obtained values were zeros, a small number of relatively very large outliers were responsible for the observed departure. It is obvious from the inset figure, were the number of zeros as a function of l_g is plotted. We can see that for the largest l_g , 96 from 100 outcomes are zeros. In this instance only one outlier was enough to cause the departure from the power law. We observe that it is in the large l_g regime where the cascade is more susceptible to the appearance of outliers (i.e., more susceptible to uniform randomness) in spite most of the results are dropping to zero. So, we also calculated $E(a_i(l_g))$ excluding 9 realizations containing at least one outlier for $g \geq 10$. The obtained result, described by the triangular points at figure 5(right), fits better to the expected power law. We interpret the presence of such outliers as indicative of the non adequacy of a uniform noise to mimic realistic fluctuations. The analysis of a critical tuning of parameters for the noise case is not accessed here. However, it is well known that the Hopf bifurcation point is postponed as a function of the noise intensity [19, 23], thus we can't rule out a critical tuning also for the stochastic situation. In fact, in light of the deterministic results, it is expected.

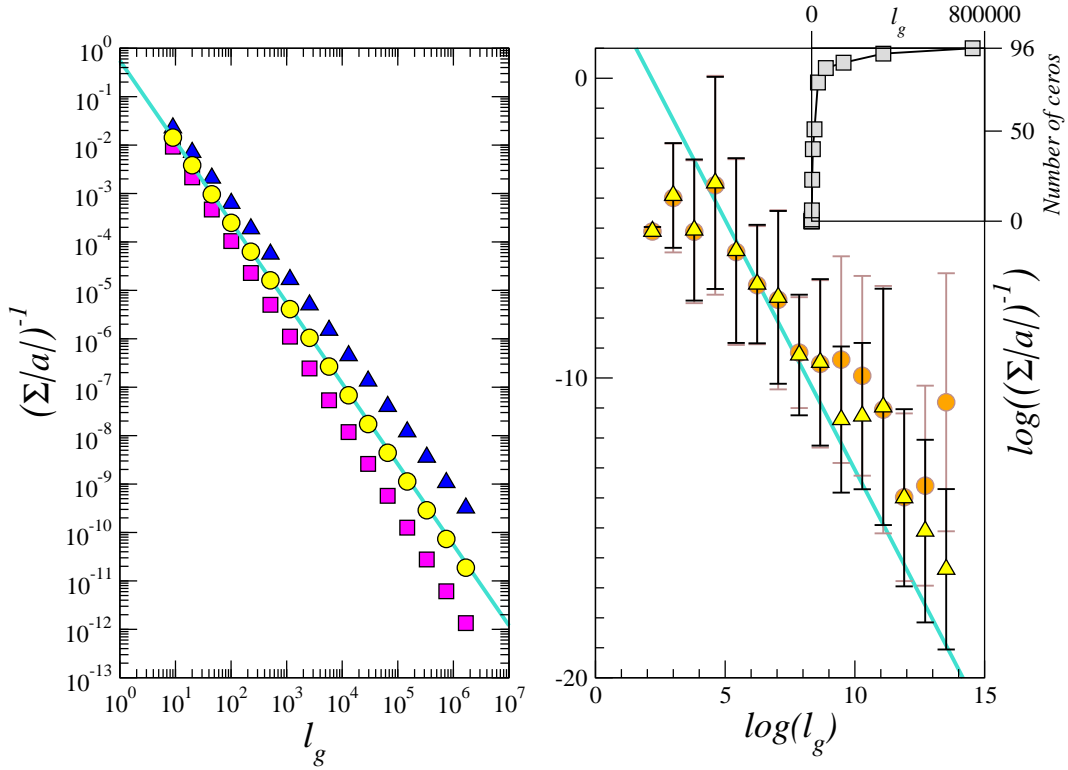


FIG. 5. In both plots the straight line is a power law with exponent $-\frac{5}{3}$. Left: Normalized results for $E(l_g) \equiv \left(\sum_{\forall a_i \neq 0} |a_i(l_g)| \right)^{-1}$. Points were calculated from the deterministic backbone with parameter values $a + b =$ (circles) $0.085 + 1.9375 = 2,0225 \sim r_H$, (triangles) $0.085 + 1.786 = 1,871 < r_H$, and (squares) $0.085 + 2.089 = 2,174 > r_H$. The power law with exponent $-\frac{5}{3}$ is reproduced when the deterministic system is almost tuned on the Hopf bifurcation critical point. Right: Results for $E(l_g) \equiv \left(\sum_{\forall a_i \neq 0} |a_i(l_g)| \right)^{-1}$, obtained when a uniformly distributed noise, η_g , is turned on. Parameter values are $r_g = a\eta_g + b$, with $a = 1.5$ and $b = 2.11$. Circles (averaging over 100 realizations) are obtained when large deviations at the tails are allowed, while triangles (averaging over 91 realizations) are for no large deviation allowed (see details in the text). Error bars represent the relative error calculated as $0.434 \frac{\sigma(E)}{E}$, with σ the standard deviation. Inset: number of obtained zero values as a function of l_g .

XIII. TIME DELAY: A BRIDGE BETWEEN THE DRM AND THE NS EQUATION

To the best of our knowledge, a direct relation between the DRM and the NS equation is not currently known. Therefore, it is up to us to sketch out such a relation. So, let's begin noticing that we can express the solutions, $\vec{u}(\vec{r}, t)$, of the incompressible form of the NS equations in terms of the Fourier representation of \vec{u} as,

$$\vec{u}(\vec{r}, t) = \sum_i x_i(t) e^{\vec{k} \cdot \vec{r}}, \quad (62)$$

thus resulting in an infinite system of ordinary differential equations for the Fourier coefficients, known as a Galerkin projection of the NS equations [27],

$$\dot{x}_i(t) = - \sum_{jk} A_{ijk} x_j(t) x_k(t) - \frac{1}{Re} |\vec{k}|^2 x_i(t) + F_i(t), \quad (63)$$

where every mode, x_i , represents a component of the velocity field with a lengthscale $|\vec{k}|$, the strength of the nonlinear interaction between modes is given by the coefficients A_{ijk} and F_i is a forcing term. Removing all but a single arbitrary wave mode, i.e., carrying out a Galerkin truncation, results in

$$\dot{x}(t) = -Ax(t)^2 - \frac{1}{Re} |\vec{k}|^2 x(t). \quad (64)$$

It is well known that this expression is not formally correct, as a mode cannot interact nonlinearly with itself. Our results seem to indicate that a better way to develop the truncation could be by keeping a single mode at two different times, i.e., requiring a time delay, τ , so to obtain

$$\dot{x}(t) = -Ax(t)x(t - \tau) - \frac{1}{Re} |\vec{k}|^2 x(t). \quad (65)$$

For an arbitrary discrete time step, Δ , it can be expressed as

$$x(t + \Delta) - x(t) = \{-Ax(t)x(t - \tau) - \frac{1}{Re} |\vec{k}|^2 x(t)\} \Delta, \quad (66)$$

Applying the temporal transformations:

$$\begin{aligned} \frac{t}{\Delta} &\rightarrow t' \\ \frac{t + \Delta}{\Delta} &\rightarrow t' + 1 \\ \frac{t - \tau}{\Delta} &\rightarrow t' - h, \end{aligned} \quad (67)$$

and providing that an integer number h exists, Eq. (66) can be rewritten as,

$$x(t+1) - x(t) = \{-Ax(t)x(t-h) - \frac{1}{Re}|\vec{k}|^2x(t)\}, \quad (68)$$

where the prime has been omitted. After rearranging terms this equation results in

$$x(t+1) = Ax(t)\left(\frac{1 - Re^{-1}|\vec{k}|^2}{A} - x(t-h)\right). \quad (69)$$

Now, requiring $\frac{1 - Re^{-1}|\vec{k}|^2}{A} = 1$, we obtain

$$x(t+1) = (1 - Re^{-1}|\vec{k}|^2)x(t)(1 - x(t-h)). \quad (70)$$

That can we expressed as

$$x_{g+1} = rx_g(1 - x_{g-h}), \quad (71)$$

where we have defined $r \equiv r_d(h)(1 - Re^{-1}|\vec{k}|^2)$, and t has been mapped to the index g . $r_d(h)$ is the control parameter value where the difference equation (71) diverges ($r_d(0) = 4$ for the case of the logistic map) so this factor allows us to obtain a range of values for r between zero and the divergence value, more information about $r_d(h)$ for different h 's can be found in [19–21]. Eq. (71) is the DRM when $h = 1$. It turns out that the inclusion of a time delay at Eq. (65) is consistent with recent findings of delayed interactions between a range of different spatial and temporal Fourier components [28, 29] and empirically deduced delayed interactions [30] in turbulence. In fact, including just one delay may fall short as the delay may increase as one goes to smaller and smaller scales [30]. This observation calls for the inclusion of several delays with changing weights [19] during the cascade, a research that is in progress.

XIV. DISCUSSION

The previous section allows us to establish a more transparent relation between x as described by Eq. (1) and the cascade coefficients. Thus, it is worth recalling that eq. (57) implies that for a given generation, let's say $g = 3$

$$\begin{aligned} \|\vec{X}_3\|^2 &\sim \Lambda_3 \\ x_3^2 + x_2^2 &\sim \Lambda_3 \\ &= (a_9 + a_8 + a_7)r_3^2 + (a_6 + a_5 + a_4)r_3 + (a_3 + a_2 + a_1). \end{aligned} \quad (72)$$

That is, the cascade intensity coefficients can be related with the sum of two components of the velocity field with neighbor lengthscales at successive generations. In particular, in the deterministic case ($r = 1$) eq. (72) becomes

$$x_3^2 + x_2^2 \sim \sum_{i=1}^9 a_i, \quad (73)$$

an expression that can be generalized as

$$x_g^2 + x_{g-1}^2 \sim \sum_{i=1}^{3^{g-1}} a_i. \quad (74)$$

or,

$$x_g \sim \sqrt{\sum_{i=1}^{3^{g-1}} a_i - x_{g-1}^2}, \quad (75)$$

i.e., a mode at scale g has information from all the coefficients at scale $g - 1$ (all of them, as 3^{g-1} is the total number of coefficients) and from the mode x_{g-1} that itself, carries information from larger scales. This transmission of information through scales is already known from the rule (49, 50) but Eq. (75) convey it in a much transparent way. Probably, this type of relationship may allows further insights about the cascading process.

Summarizing, here the $-5/3$ power law was obtained with an exact calculation and not using a numerical approach. It takes us to the question whether turbulence energy cascades could be governed by an analytical structure at least similar to rule (49, 50) or whether it may require the inclusion of several delays, in which case the effect on the cascading analytical rule and on scaling has to be clarified. Some preliminary work seem to show that a generalization of the rule can be obtained for extended and combined values of the memory h .

We would like to finish noticing that these results add further evidence of the relevance of low dimensional discrete dynamics to understand complex phenomena [2] and turbulence, in particular. As intermittency and non-Gaussian statistics can be observed in many complex systems [31, 32], it also may be the case for $-5/3$ turbulent cascades. Here it is shown that this cascade is not exclusive for fluids but a dynamical state rooted solely in critical deterministic nonlinear dynamics. In particular, Eq. (1) is a specific case of a Lotka-Volterra system, known to hold a winnerless competition [33] based on a multifractal neural coding scheme, which provides the first intrinsic neuro-dynamical explanation for wandering animal behavior [34]. Also, Eq. (1) can be related to SIR epidemic transmission dynamics [35]. One

may conjecture that these two systems could also experience complex cascading phenomena of some kind, in nervous information processing in a case and in epidemic propagation in the other.

XV. ACKNOWLEDGEMENTS

We thank Juan S. Medina-Álvarez for useful comments and discussions. JLCF and EDG acknowledges support from IVIC-141 grant during a small part of this work and personal support from Prof. M. C. Pereyra (UNM).

XVI. AUTHOR CONTRIBUTIONS STATEMENT

JLCF conceived, directed, and developed all aspects of this research. MRM contributed with software development and simulation validations, EG independently validated the analytics. All authors contributed to paper writing. The authors declare no competing financial interests.

XVII. ADDITIONAL INFORMATION

Correspondence and requests for materials should be addressed to JLCF.

Appendix A: Eigenvalues of p_2

Let's calculate the second inner product, given by,

$$\begin{aligned}
 p_2 &\equiv \mathbf{A}_{g-2}^\dagger p_1 \mathbf{A}_{g-2} = & (A1) \\
 &= \begin{bmatrix} \frac{r_2}{\beta} & 1 \\ -\alpha r_2 & 0 \end{bmatrix} \begin{bmatrix} \frac{r_1^2 + \beta^2}{\beta^2} & -\frac{r_1^2}{\beta} \alpha \\ -\frac{r_1^2}{\beta} \alpha & \alpha^2 r_1^2 \end{bmatrix} \begin{bmatrix} \frac{r_2}{\beta} & -\alpha r_2 \\ 1 & 0 \end{bmatrix} = \\
 &= \begin{bmatrix} \frac{r_2^2 r_1^2 + r_2^2 \beta^2 - 2r_2 r_1^2 \alpha \beta^2 + r_1^2 \alpha^2 \beta^4}{\beta^4} & \frac{-r_2 r_1^2 - r_2 \beta^2 + r_1^2 \alpha \beta^2}{\beta^3} \alpha r_2 \\ \frac{-r_2 r_1^2 - r_2 \beta^2 + r_1^2 \alpha \beta^2}{\beta^3} \alpha r_2 & \alpha^2 r_2^2 \frac{r_1^2 + \beta^2}{\beta^2} \end{bmatrix},
 \end{aligned}$$

with eigenvalues,

$$\lambda_{\pm}^{p_2} = \frac{1}{2\beta^4} (r_2^2 r_1^2 + r_2^2 \beta^2 - 2r_2 r_1^2 \alpha \beta^2 + \beta^4 \alpha^2 r_1^2 + \beta^2 \alpha^2 r_2^2 r_1^2 + \beta^4 \alpha^2 r_2^2 \pm$$

$$\begin{aligned}
& (2r_2^4 r_1^2 \beta^2 + r_2^4 r_1^4 + r_2^4 \beta^4 + 2r_2^4 \beta^6 \alpha^2 + \beta^8 \alpha^4 r_1^4 + \beta^8 \alpha^4 r_2^4 - 4r_2 r_1^4 \alpha^3 \beta^6 \\
& - 4r_2^3 r_1^4 \alpha^3 \beta^4 - 4r_2^3 r_1^2 \alpha^3 \beta^6 + 2\beta^6 \alpha^4 r_1^4 r_2^2 + \beta^4 \alpha^4 r_2^4 r_1^4 + 2\beta^6 \alpha^4 r_2^4 r_1^2 \\
& - 2\beta^8 \alpha^4 r_1^2 r_2^2 - 4r_2^3 r_1^4 \alpha \beta^2 + 6r_2^2 r_1^4 \beta^4 \alpha^2 + 2r_2^4 r_1^4 \beta^2 \alpha^2 + 4r_2^4 r_1^2 \beta^4 \alpha^2 \\
& - 4r_2^3 \beta^4 r_1^2 \alpha + 2r_2^2 \beta^6 \alpha^2 r_1^2)^{1/2}. \tag{A2}
\end{aligned}$$

Here, we can define,

$$\Lambda_2 \equiv \left[\begin{array}{c} (1 + \beta^2 \alpha^2) r_1^2 \\ + (\beta^2 + \beta^4 \alpha^2) \end{array} \right] r_2^2 + \left[(-2\alpha\beta^2) r_1^2 \right] r_2 + \left[(\beta^4 \alpha^2) r_1^2 \right]. \tag{A3}$$

It is easy to show that the term under the square root differs from Λ_2 by $4\alpha^4 r_2^2 r_1^2 \beta^8$. Then, we can make use of $\Upsilon_2 \equiv \sqrt{4\alpha^4 r_2^2 r_1^2 \beta^8} = 2\beta^4 \alpha^2 r_2 r_1$, to write the eigenvalues of p_2 as $\lambda_{\pm}^{p_2} = \frac{1}{2\beta^4} \left(\Lambda_2 \pm \sqrt{\Lambda_2^2 - \Upsilon_2^2} \right)$.

Appendix B: Eigenvalues of p_3

The third inner product, given by,

$$\begin{aligned}
p_3 &= \mathbf{A}_{g-3}^\dagger p_2 \mathbf{A}_{g-3} = \tag{B1} \\
&= \mathbf{A}_{g-3} \left[\begin{array}{cc} \frac{r_2^2 r_1^2 + r_2^2 \beta^2 - 2r_2 r_1^2 \alpha \beta^2 + r_1^2 \alpha^2 \beta^4}{\beta^4} & \frac{-r_2 r_1^2 - r_2 \beta^2 + r_1^2 \alpha \beta^2}{\beta^3} \alpha r_2 \\ \frac{-r_2 r_1^2 - r_2 \beta^2 + r_1^2 \alpha \beta^2}{\beta^3} \alpha r_2 & \alpha^2 r_2^2 \frac{r_1^2 + \beta^2}{\beta^2} \end{array} \right] \mathbf{A}_{g-3},
\end{aligned}$$

has eigenvalues that can be written as $\lambda_{\pm}^{p_3} = \frac{1}{2\beta^6} \left(\Lambda_3 \pm \sqrt{\Lambda_3^2 - \Upsilon_3^2} \right)$, where,

$$\begin{aligned}
\Lambda_3 &\equiv \left\{ \begin{array}{l} \left[\begin{array}{c} (1 + \beta^2 \alpha^2) r_1^2 \\ + (\beta^2 + \beta^4 \alpha^2) \end{array} \right] r_2^2 \\ + \left[(-2\alpha\beta^2 - 2\beta^4 \alpha^3) r_1^2 \right] r_2 \\ + \left[(\beta^4 \alpha^2 + \beta^6 \alpha^4) r_1^2 \right] \end{array} \right\} r_3^2 + \tag{B2} \\
&+ \left\{ \begin{array}{l} \left[(-2\alpha\beta^2) r_1^2 \right] \\ + (-2\alpha\beta^4) \end{array} \right\} r_2^2 \\
&+ \left[(2\alpha^2 \beta^4) r_1^2 \right] r_2 \\
&+ \left\{ \begin{array}{l} \left[(\beta^4 \alpha^2) r_1^2 \right] \\ + (\alpha^2 \beta^6) \end{array} \right\} r_2^2
\end{aligned}$$

and $\Upsilon_3 = 2\beta^6 \alpha^3 r_3 r_2 r_1$.

Appendix C: Eigenvalues of p_4

The fourth inner product becomes,

$$p_4 = \mathbf{A}_{g-4}^\dagger p_3 \mathbf{A}_{g-4} \quad (\text{C1})$$

with eigenvalues $\lambda_{\pm}^{p_4} = \frac{1}{2\beta^8} \left(\Lambda_4 \pm \sqrt{\Lambda_4^2 - \Upsilon_4^2} \right)$, where,

$$\Lambda_4 \equiv \left(\left(\left\{ \begin{array}{l} \left[(1 + \beta^2 \alpha^2) r_1^2 \right] \\ + (\beta^2 + \beta^4 \alpha^2) \end{array} \right\} r_2^2 \right) \right. \\ \left. + \left\{ \begin{array}{l} \left[(-2 \beta^4 \alpha^3 - 2 \alpha \beta^2) r_1^2 \right] \\ + \left[(\beta^6 \alpha^4 + \beta^4 \alpha^2) r_1^2 \right] \end{array} \right\} r_2 \right\} r_3^2 \\ + \left\{ \begin{array}{l} \left[(-2 \beta^4 \alpha^3 - 2 \alpha \beta^2) r_1^2 \right] \\ + (-2 \beta^6 \alpha^3 - 2 \alpha \beta^4) \\ + \left[(2 \beta^6 \alpha^4 + 2 \beta^4 \alpha^2) r_1^2 \right] \end{array} \right\} r_2 \right\} r_3 \\ + \left\{ \begin{array}{l} \left[(\beta^6 \alpha^4 + \beta^4 \alpha^2) r_1^2 \right] \\ + (\beta^8 \alpha^4 + \alpha^2 \beta^6) \end{array} \right\} r_2^2 \right) \\ + \left(\left(\left\{ \begin{array}{l} \left[(-2 \alpha \beta^2) r_1^2 \right] \\ + (-2 \alpha \beta^4) \end{array} \right\} r_2^2 \right) \right. \\ \left. + \left\{ \begin{array}{l} \left[(4 \alpha^2 \beta^4) r_1^2 \right] \\ + \left[(-2 \alpha^3 \beta^6) r_1^2 \right] \end{array} \right\} r_2 \right\} r_3^2 \\ + \left\{ \begin{array}{l} \left[(2 \beta^4 \alpha^2) r_1^2 \right] \\ + (2 \alpha^2 \beta^6) \\ + \left[(-2 \alpha^3 \beta^6) r_1^2 \right] \end{array} \right\} r_2 \right\} r_3 \\ + \left(\left(\left\{ \begin{array}{l} \left[(\beta^4 \alpha^2) r_1^2 \right] \\ + (\alpha^2 \beta^6) \end{array} \right\} r_2^2 \right) \right. \\ \left. + \left\{ \begin{array}{l} \left[(-2 \alpha^3 \beta^6) r_1^2 \right] \\ + \left[(\alpha^4 \beta^8) r_1^2 \right] \end{array} \right\} r_2 \right\} r_3^2 \right) \right) \quad (\text{C2})$$

and $\Upsilon_4 = 2\beta^8 \alpha^4 r_4 r_3 r_2 r_1$.

Appendix D: Eigenvalues of p_5

Here we show p_5 , given by,

$$p_5 = \mathbf{A}_{g-5}^\dagger p_4 \mathbf{A}_{g-5}, \quad (\text{D1})$$

with eigenvalues, $\lambda_{\pm}^{p_5} = \frac{1}{2\beta^{10}} \left(\Lambda_5 \pm \sqrt{\Lambda_5^2 - \Upsilon_5^2} \right)$, with,

$$\Lambda_5 \equiv \left[\begin{array}{l} \left(\left\{ \begin{array}{l} \left[(1 + \beta^2 \alpha^2) r_1^2 \right] r_2^2 \\ + (\beta^2 + \beta^4 \alpha^2) \end{array} \right\} r_2^2 \right. \\ \left. + \left\{ \begin{array}{l} \left[(-2\alpha\beta^2 - 2\beta^4\alpha^3) r_1^2 \right] r_2 \\ + \left[(\beta^4\alpha^2 + \beta^6\alpha^4) r_1^2 \right] \end{array} \right\} r_3^2 \right. \\ \left. + \left\{ \begin{array}{l} \left[(-2\alpha\beta^2 - 2\beta^4\alpha^3) r_1^2 \right] r_2^2 \\ + (-2\beta^6\alpha^3 - 2\alpha\beta^4) \end{array} \right\} r_3 \right. \\ \left. + \left\{ \begin{array}{l} \left[(2\beta^6\alpha^4 + 2\beta^4\alpha^2) r_1^2 \right] r_2 \\ + \left\{ \begin{array}{l} \left[(\beta^4\alpha^2 + \beta^6\alpha^4) r_1^2 \right] r_2^2 \\ + (\beta^8\alpha^4 + \alpha^2\beta^6) \end{array} \right\} \end{array} \right\} r_4^2 \right) \\ + \left(\left\{ \begin{array}{l} \left[(-2\alpha\beta^2 - 2\beta^4\alpha^3) r_1^2 \right] r_2^2 \\ + (-2\beta^6\alpha^3 - 2\alpha\beta^4) \end{array} \right\} r_3^2 \right. \\ \left. + \left\{ \begin{array}{l} \left[(4\beta^6\alpha^4 + 4\beta^4\alpha^2) r_1^2 \right] r_2 \\ + \left[(-2\beta^6\alpha^3 - 2\beta^8\alpha^5) r_1^2 \right] \end{array} \right\} r_4 \right. \\ \left. + \left\{ \begin{array}{l} \left[(2\beta^6\alpha^4 + 2\beta^4\alpha^2) r_1^2 \right] r_2^2 \\ + (2\beta^8\alpha^4 + 2\alpha^2\beta^6) \end{array} \right\} r_3 \right. \\ \left. + \left(\left\{ \begin{array}{l} \left[(\beta^4\alpha^2 + \beta^6\alpha^4) r_1^2 \right] r_2^2 \\ + (\beta^8\alpha^4 + \alpha^2\beta^6) \end{array} \right\} r_3^2 \right. \right. \\ \left. \left. + \left\{ \begin{array}{l} \left[(-2\beta^6\alpha^3 - 2\beta^8\alpha^5) r_1^2 \right] r_2 \\ + \left[(\beta^8\alpha^4 + \beta^{10}\alpha^6) r_1^2 \right] \end{array} \right\} r_3^2 \right) \right) \end{array} \right] r_5^2 \quad (\text{D2})$$

$$\begin{aligned}
& + \left[\left(\left\{ \begin{aligned} & \left[\begin{array}{l} (-2\alpha\beta^2)r_1^2 \\ + (-2\alpha\beta^4) \end{array} \right] r_2^2 \\ & + \left[\begin{array}{l} (4\alpha^2\beta^4)r_1^2 \\ (-2\alpha^3\beta^6)r_1^2 \end{array} \right] r_2 \end{aligned} \right\} r_3^2 \\ & + \left\{ \begin{aligned} & \left[\begin{array}{l} (4\beta^4\alpha^2)r_1^2 \\ + (4\alpha^2\beta^6) \end{array} \right] r_2^2 \\ & + \left[\begin{array}{l} (-4\alpha^3\beta^6)r_1^2 \\ (-2\alpha^3\beta^8) \end{array} \right] r_2 \end{aligned} \right\} r_3 + \\ & + \left\{ \begin{aligned} & \left[\begin{array}{l} (-2\alpha^3\beta^6)r_1^2 \\ (-2\alpha^3\beta^8) \end{array} \right] r_2^2 \\ & + \left[\begin{array}{l} (2\beta^4\alpha^2)r_1^2 \\ + (2\alpha^2\beta^6) \end{array} \right] r_2^2 \\ & + \left[\begin{array}{l} (-4\alpha^3\beta^6)r_1^2 \\ + (2\alpha^4\beta^8)r_1^2 \end{array} \right] r_2 \end{aligned} \right\} r_4 \\ & + \left\{ \begin{aligned} & \left[\begin{array}{l} (-2\alpha^3\beta^6)r_1^2 \\ + (-2\alpha^3\beta^8) \end{array} \right] r_2^2 \\ & + \left[\begin{array}{l} (2\alpha^4\beta^8)r_1^2 \end{array} \right] r_2 \end{aligned} \right\} r_3 \end{aligned} \right) \right] r_5 \\
& + \left[\left(\left\{ \begin{aligned} & \left[\begin{array}{l} (\beta^4\alpha^2)r_1^2 \\ + (\alpha^2\beta^6) \end{array} \right] r_2^2 \\ & + \left[\begin{array}{l} (-2\alpha^3\beta^6)r_1^2 \\ + (\alpha^4\beta^8)r_1^2 \end{array} \right] r_2 \end{aligned} \right\} r_3^2 \\ & + \left\{ \begin{aligned} & \left[\begin{array}{l} (-2\alpha^3\beta^6)r_1^2 \\ + (-2\alpha^3\beta^8) \end{array} \right] r_2^2 \\ & + \left[\begin{array}{l} (2\alpha^4\beta^8)r_1^2 \end{array} \right] r_2 \end{aligned} \right\} r_3 \\ & + \left\{ \begin{aligned} & \left[\begin{array}{l} (\alpha^4\beta^8)r_1^2 \\ + (\alpha^4\beta^{10}) \end{array} \right] r_2^2 \end{aligned} \right\} \end{aligned} \right) \right] r_4^2
\end{aligned}$$

and $\Upsilon_5 = 2\beta^{10}\alpha^5r_5r_4r_3r_2r_1$.

[1] J. P. Eckmann, Rev. Mod. Phys. **53**, 643 (1981).

[2] L. P. Kadanoff, Physics Today **36**, 46 (1983).

- [3] T. Bohr, M. H. Jensen, G. Paladin, and A. Vulpiani, *Dynamical Systems Approach to Turbulence* (Cambridge University Press, Cambridge, 1998).
- [4] U. Frisch, *Turbulence: The Legacy of A. N. Kolmogorov* (Cambridge University Press, 1995).
- [5] J. M. McDonough, Phys. Rev. E **79**, 065302 (2009).
- [6] R. M. May, Nature **261**, 459 (1976).
- [7] M. J. Feigenbaum, Communications in Mathematical Physics **77**, 65 (1980).
- [8] Libchaber, A. and Maurer, J., J. Phys. Colloques **41**, 51 (1980).
- [9] L. F. Richardson, Proceedings of the Royal Society of London Series A **110**, 709 (1926).
- [10] A. N. Kolmogorov, Soviet Physics Uspekhi **10**, 734 (1968).
- [11] L. Onsager, Phys. Rev. **68**, 286 (1945).
- [12] A. M. Obukhov, Dok. Akad. Nauk. SSSR **32**, 22 (1941).
- [13] W. Heisenberg, Zeitschrift für Physik **124**, 628 (1948).
- [14] C. F. v. Weizsäcker, Zeitschrift für Physik **124**, 614 (1948).
- [15] J. Maynard Smith, *Mathematical Ideas in Biology* (Cambridge University Press, 1968).
- [16] D. G. Aronson, M. A. Chory, G. R. Hall, and R. P. McGehee, Communications in Mathematical Physics **83**, 303 (1982).
- [17] J. R. Pounder and T. D. Rogers, Bulletin of Mathematical Biology **42**, 551 (1980).
- [18] Y. Morimoto, Physics Letters A **134**, 179 (1988).
- [19] J. L. Cabrera, *Contribución a la descripción estocástica de algunos sistemas dinámicos no lineales con retardo temporal*, Ph.D. thesis, U.N.E.D, Madrid, Spain (1997).
- [20] J. L. Cabrera and F. J. de la Rubia, Physics Letters A **197**, 19 (1995).
- [21] J. L. Cabrera and F. J. de la Rubia, International Journal of Bifurcation and Chaos **06**, 1683 (1996).
- [22] J. L. Cabrera and F. J. d. l. Rubia, Europhys. Lett. **39**, 123 (1997).
- [23] J. L. Cabrera, J. Gorroñoigoitia, and F. J. de la Rubia, Phys. Rev. Lett. **82**, 2816 (1999).
- [24] V. Trifonov, L. Pasqualucci, R. Dalla-Favera, and R. Rabadan, Scientific Reports **1**, 191 (2011).
- [25] S. G. Saddoughi and S. V. Veeravalli, J. Fluid Mechanics **268**, 333 (1994).
- [26] G. L. Eyink and K. R. Sreenivasan, Rev. Mod. Phys. **78**, 87 (2006).
- [27] G. Flierl and R. Ferrari, Turbulence in the Ocean and Atmosphere. MIT OpenCourseWare. <https://ocw.mit.edu>. (2006).

- [28] M. Dotti, R. Schlander, P. Buchhave, and C. M. Velte, Experimental investigation of the turbulent cascade development by injection of single large-scale fourier modes (2020).
- [29] P. Buchhave and C. M. Velte, Dynamic triad interactions and evolving turbulence spectra (2021), arXiv:1906.04756 [physics.flu-dyn].
- [30] C. Josserand, M. Le Berre, T. Lehner, and Y. Pomeau, *Journal of Statistical Physics* **167**, 596 (2017).
- [31] J. L. Cabrera and J. G. Milton, *Chaos: An Interdisciplinary Journal of Nonlinear Science* **14**, 691 (2004).
- [32] R. N. Mantegna and H. E. Stanley, *Nature* **376**, 46 (1995).
- [33] L. A. González-Díaz, E. D. Gutiérrez, P. Varona, and J. L. Cabrera, *Phys. Rev. E* **88**, 012709 (2013).
- [34] E. D. Gutiérrez and J. L. Cabrera, *Scientific Reports* **5**, 18009 (2015).
- [35] L. J. Allen, *Mathematical Biosciences* **124**, 83 (1994).